Progressive Source and Reaction Fields for Magnetodynamic Model Refinement via a Finite Element Subproblem Method

Patrick Dular[1,2], Mauricio V. Ferreira da Luz[3], Patrick Kuo-Peng[3] and Laurent Krähenbühl[4]

[1] University of Liege, Dept. of Electrical Engineering and Computer Science, ACE, Belgium [2] F.R.S.-FNRS, Belgium
[3] Universidade Federal de Santa Catarina, GRUCAD, Brazil
[4] Université de Lyon, Ampère (CNRS UMR5005), École Centrale de Lyon, France

***Abstract*—Magnetodynamic models are split into a sequence of progressive finite element subproblems. The source fields generated by the active conductors alone are calculated at first via either finite elements or the Biot-Savart law. The associated reaction fields for each added magnetic and/or conducting region, and in return for the source regions themselves when massive, are then calculated with finite element models, possibly with initial perfect magnetic, conductor and/or impedance boundary conditions to be further corrected. The resulting subproblem method allows efficient solving of parameterized analyses thanks to a proper mesh for each subproblem and the reuse of previous solutions to be locally corrected. Accuracy improvements are obtained for local fields and global quantities, i.e. inductances, resistances, Joule losses and forces.**

Keywords—Eddy currents; finite element method; model refinement; subproblem method.

I. Introduction

Instead of solving a complete magnetodynamic problem, including all conducting and magnetic regions, it is here proposed to perform successive finite element (FE) calculations via a subproblem (SP) method (SPM) [1]-[6], mainly by separating the regions, with the advantage of using a different mesh at each step, or no mesh when the Biot-Savart law is used. Source and reaction fields are considered but, at the difference with the common method that adds these fields in the whole domain to define the total field, the source fields are here to be defined only in the added regions [3]-[5]. Such a support reduction is of importance for efficient calculations, especially for source fields calculated via the Biot-Savart law.

When acting as volume sources (VSs) in each added region, the source fields can be even initially reduced to its boundary, which is an important and useful aspect developed here. Instead of volume projections of the source fields in the mesh of the added region the source fields are rather calculated there, as a first alternative, via a FE problem with their boundary values as boundary conditions (BCs). Another general alternative aims at avoiding any source field volume projection or calculation thanks to interface conditions (ICs).

Intermediary SPs can tackle the added regions at various levels of precision, e.g. considering the magnetic regions via perfect magnetic material BCs, or the conducting/magnetic regions via perfect conductor or impedance BCs [1]-[2], thus with the source fields acting as surface sources (SSs). Avoiding to mesh their interior allows to lighten the computational efforts, which is interesting for the preliminary stage of a design. Perfect conductor BCs are suitable for high conductivities or frequencies, i.e. for low skin depths [2]. For larger skin depths, impedance BCs (IBCs) lead to a better accuracy but, as they are generally based on analytical solutions of ideal problems, they are only valid in practice far from geometrical discontinuities, e.g., edges and corners. An additional SP is then of interest to correct these surface models with approximate BCs to volume models [6]. Sequences of such SP solutions and/or corrections are developed for the magnetic vector potential FE magnetodynamic formulation. They are illustrated on application examples.

II. Coupled Subproblems

A. Sequence of Subproblems

To allow a progression from simple to more elaborate models, a complete problem is split into a series of SPs that define a sequence of changes, with the complete or total solution given by the sum of the SP solutions [3]-[5]. Each SP is defined in its particular domain, generally distinct from the complete one and usually overlapping those of the other SPs. At the discrete level, this aims to decrease the problem complexity and to allow distinct meshes with suitable refinements and possible domain overlapping between SPs.

B. Canonical Form of Magnetodynamic Subproblems

A canonical magnetodynamic SP p, to be solved at step p of the SPM, is defined in a domain Ω_p, with boundary $\partial\Omega_p = \Gamma_p = \Gamma_{h,p} \cup \Gamma_{b,p}$. The eddy current conducting part of Ω_p is denoted $\Omega_{c,p}$ and the non-conducting one $\Omega_{c,p}^C$, with $\Omega_p = \Omega_{c,p} \cup \Omega_{c,p}^C$. Massive conductors belong to $\Omega_{c,p}$, whereas stranded conductors belong to $\Omega_{s,p} \subset \Omega_{c,p}^C$. The equations, material relations and BCs of SP p are

$$\mathrm{curl}\,\boldsymbol{h}_p = \boldsymbol{j}_p\,,\quad \mathrm{div}\,\boldsymbol{b}_p = 0\,,\quad \mathrm{curl}\,\boldsymbol{e}_p = -\partial_t \boldsymbol{b}_p\,, \qquad \text{(1a-b-c)}$$

$$\boldsymbol{h}_p = \mu_p^{-1}\,\boldsymbol{b}_p + \boldsymbol{h}_{s,\mathrm{p}}\,,\quad \boldsymbol{j}_p = \sigma_p\,\boldsymbol{e}_p + \boldsymbol{j}_{s,\mathrm{p}}\,, \qquad \text{(2a-b)}$$

$$\boldsymbol{n}\times\boldsymbol{h}_p|_{\Gamma_{h,p}} = \boldsymbol{j}_{f,p}\,,\ \boldsymbol{n}\cdot\boldsymbol{b}_p|_{\Gamma_{b,p}} = \boldsymbol{f}_{f,p}\,,\ \boldsymbol{n}\times\boldsymbol{e}_p|_{\Gamma_{e,p}\subset\Gamma_{b,p}} = \boldsymbol{k}_{f,p}\,, \qquad \text{(3a-b-c)}$$

where $\boldsymbol{h}_p$ is the magnetic field, $\boldsymbol{b}_p$ is the magnetic flux density, $\boldsymbol{e}_p$ is the electric field, $\boldsymbol{j}_p$ is the electric current density, μ_p is the magnetic permeability, σ_p is the electric conductivity, $\boldsymbol{n}$ is the unit normal on Γ_p exterior to Ω_p and $\boldsymbol{j}_{f,p}$, $\boldsymbol{f}_{f,p}$ and $\boldsymbol{k}_{f,p}$ are some given surface fields, defining SSs. Note that (1c) is only defined in $\Omega_{c,p}$ (as well as $\boldsymbol{e}_p$), whereas it is reduced to (1b) in $\Omega_{c,p}{}^C$.

Fields $\boldsymbol{h}_{s,\mathrm{p}}$ and $\boldsymbol{j}_{s,\mathrm{p}}$ in (2a-b) are VSs. They can classically be remnant fields in magnets or fixed current densities in conductors. With the SPM, $\boldsymbol{h}_{s,p}$ is also used for expressing changes of permeability and $\boldsymbol{j}_{s,p}$ for changes of conductivity [3], [4]. For changes from μ_q and σ_q for previous SP q to μ_p and σ_p for SP p in some regions, the associated VSs $\boldsymbol{h}_{s,p}$ and $\boldsymbol{j}_{s,p}$, nonzero only in these regions, are

$$\boldsymbol{h}_{s,p} = (\mu_p^{-1} - \mu_q^{-1})\,\boldsymbol{b}_q\,,\quad \boldsymbol{j}_{s,p} = (\sigma_p - \sigma_q)\,\boldsymbol{e}_q\,. \qquad \text{(4a-b)}$$

These correctly define the material relations for the total fields, i.e., $\boldsymbol{h}_q + \boldsymbol{h}_p = \mu_p^{-1}\,(\boldsymbol{b}_q + \boldsymbol{b}_p)$ and $\boldsymbol{j}_q + \boldsymbol{j}_p = \sigma_p\,(\boldsymbol{e}_q + \boldsymbol{e}_p)$.

Regarding BCs (3a-b-c), some paired portions of Γ_p can define double layers, with the thin region in between exterior to Ω_p [1]-[6]. In particular, these will be associated with the boundary of regions initially considered, in previous SP q, via simplified BCs. They are denoted γ_p^+ and γ_p^- and are geometrically defined as a single surface γ_p with ICs, fixing the discontinuities or IC-SSs ($[\,\cdot\,]_{\gamma_p} = \cdot\,|_{\gamma_p^+} - \cdot\,|_{\gamma_p^-}$), i.e.,

$$[\boldsymbol{n}\times\boldsymbol{h}_p]_{\gamma_p} = [\boldsymbol{j}_{f,p}]_{\gamma_p},\ [\boldsymbol{n}\cdot\boldsymbol{b}_p]_{\gamma_p} = [\boldsymbol{f}_{f,p}]_{\gamma_p},\ [\boldsymbol{n}\times\boldsymbol{e}_p]_{\gamma_p} = [\boldsymbol{k}_{f,p}]_{\gamma_p}. \qquad \text{(5a-b-c)}$$

C. Canonical Magnetic Vector Potential Weak Formulation

The magnetic vector potential $\boldsymbol{a}_p$ and the electric scalar potential v_p are defined via

$$\boldsymbol{b}_p = \mathrm{curl}\,\boldsymbol{a}_p\,,\quad \boldsymbol{e}_p = -\partial_t \boldsymbol{a}_p - \mathrm{grad}\,v_p = -\partial_t \boldsymbol{a}_p - \boldsymbol{u}_p, \qquad \text{(6a-b)}$$

$$\boldsymbol{n}\times\boldsymbol{a}_p|_{\Gamma_{b,p}} = \boldsymbol{a}_{f,p}\,,\quad [\boldsymbol{n}\times\boldsymbol{a}_p]_{\gamma_p} = [\boldsymbol{a}_{f,p}]_{\gamma_p}, \qquad \text{(7a-b)}$$

with given surface potential $\boldsymbol{a}_{f,p}$. The $\boldsymbol{a}_p$ weak formulation of the magnetodynamic problem is then obtained from the weak form of the Ampère equation, i.e. [3],

$$\begin{aligned}&(\mu_p^{-1}\,\mathrm{curl}\,\boldsymbol{a}_p, \mathrm{curl}\,\boldsymbol{a}')_{\Omega_p} + (\boldsymbol{h}_{s,p}, \mathrm{curl}\,\boldsymbol{a}')_{\Omega_p} - (\boldsymbol{j}_{s,p}, \boldsymbol{a}')_{\Omega_p}\\ &+ (\sigma_p\,\partial_t \boldsymbol{a}_p, \boldsymbol{a}')_{\Omega_{c,p}} + (\sigma_p\,\boldsymbol{u}_p, \boldsymbol{a}')_{\Omega_{c,p}} + <\boldsymbol{n}\times\boldsymbol{h}_p, \boldsymbol{a}'>_{\Gamma_{h,p}\setminus\gamma_p}\\ &+ <[\boldsymbol{n}\times\boldsymbol{h}_p]_{\gamma_p}, \boldsymbol{a}'>_{\gamma_p} = 0\,,\ \forall \boldsymbol{a}' \in F_p^1(\Omega_p),\end{aligned} \qquad \text{(8)}$$

where $F_p{}^1(\Omega_p)$ is a curl-conform function space defined on Ω_p, gauged in $\Omega_{c,p}{}^C$, and containing the basis functions for $\boldsymbol{a}_p$ and for the test function $\boldsymbol{a}'$ (at the discrete level, this space is defined by edge FEs; the gauge is based on the tree-co-tree technique); $(\,\cdot\,,\cdot\,)_\Omega$ and $<\cdot\,,\cdot>_\Gamma$ denote a volume integral in Ω and a surface integral on Γ, respectively, of the product of their field arguments. An SP p with only sources $\boldsymbol{j}_{s,\mathrm{p}}$ in $\Omega_{s,p}$ has a direct solution given by the Biot-Savart formula, with no need of FE calculation.

D. Addition of Material Regions with Model Refinements

Progressively adding some material regions, a wide variety of SPs can be defined to allow various source and reaction fields, together with model refinements of the added regions. Each SP p is defined as a change or correction of a previous (or several) SP(s) q, $\forall\, q < p$ (i.e., for all SPs q prior to SP p), without involving the already considered sources (i.e., active conductors, previous VSs and SSs). It is constrained via VSs and SSs defined from parts of the solutions of the SP(s) q, as detailed hereafter for practical models.

A change with a significant effect on the previously solved SPs has to be further considered as a source for these, which thus requires iterative corrections. Also, a nonlinear SP p requires classical nonlinear iterations.

E. Required Sources and their Discretization via Projections

Each SP p requires VSs and/or SSs in some regions $\omega_{s,p}\subset\Omega_p$ evaluated from previous SPs q, $\forall\, q < p$. These sources, coming from previous meshes or Biot-Savart evaluations of SPs q, have to be properly discretized in the mesh of SP p to assure the conformity of the sequenced FE weak formulations. They are obtained by means of Galerkin projections [10] of the primary field $\boldsymbol{a}_q$ between the meshes, i.e.

$$(\mathrm{curl}\,\boldsymbol{a}_{q,p\text{-}mesh}, \mathrm{curl}\,\boldsymbol{a}')_{\omega_{s,p}} = (\mathrm{curl}\,\boldsymbol{a}_q, \mathrm{curl}\,\boldsymbol{a}')_{\omega_{s,p}}, \forall \boldsymbol{a}' \in F_p^1(\omega_{s,p}), \qquad \text{(9)}$$

where $F_p{}^1(\omega_{s,p})$ is a gauged curl-conform function space for the projected source $\boldsymbol{a}_{q,p\text{-}mesh}$ (the projection of $\boldsymbol{a}_q$ on mesh p) and the test function $\boldsymbol{a}'$.

SSs associated with $\boldsymbol{n}\times\boldsymbol{h}_q|_{\Gamma_{h,p,i}}$, with (3a) or (5a), are involved in surface integral terms in (8) for SP p. Being of weak nature, they are to be weakly expressed from (8) written for each prior SP q, $\forall\, q < p$, i.e. from volume integrals generally limited to

$$<\boldsymbol{n}\times\boldsymbol{h}_q, \boldsymbol{a}'>_{\Gamma_{h,p,i}} = -(\mu_q^{-1}\,\mathrm{curl}\,\boldsymbol{a}_q, \mathrm{curl}\,\boldsymbol{a}')_{\Omega_p = \Omega_q}\,. \qquad \text{(10)}$$

At the discrete level, the volume integral in (10) is limited to one single layer of FEs touching $\Gamma_{h,p,i}$ (thus on one side of $\Gamma_{h,p,i}$), because it involves only the associated trace $\boldsymbol{n}\times\boldsymbol{a}'|_{\Gamma_{h,p,i}}$. The source $\boldsymbol{a}_q$, initially in the mesh of SP q, has to be projected in the mesh of SP p via (9) only in the FE layer as the projection region $\omega_{s,p}$, which thus decreases the computational effort of the projection process.

SSs associated with $\boldsymbol{n}\cdot\boldsymbol{b}_q|_{\Gamma_{b,p,i}}$, with (3b-c), (5b-c) or (7a-b), are of strong nature. They are to be directly defined in function space $F_p^{\,1}(\Omega_p)$, with source $\boldsymbol{a}_q$ to be projected only on $\Gamma_{b,p,i}$, or at most in a FE layer touching $\Gamma_{b,p,i}$.

III. Progressive Models as SPs

A. Active Conductor with FEs (COND-FE) or Biot-Savart (COND-BS) Formula

Considering each active conductor $\Omega_{s,p}$ or $\Omega_{c,p}$, fed by external circuits, without any other region in a domain Ω_p, with some possible symmetries that do not exist anymore in the complete problem, offers advantages in mesh operations, especially in parameterized analyzes on positions and dimensions. The field it generates can serve as a source field for further SPs. It can be calculated via an FE SP $p \equiv$ *COND-FE* in the mesh of Ω_p [3] (Fig. 2). It can also be calculated via the Biot-Savart formula [9] with a given $\boldsymbol{j}_{s,p}$ (even initially applied to a simplified wire geometry of $\Omega_{s,p}$), being a direct solution of this SP $p \equiv$ *COND-BS*. BS source fields $\boldsymbol{b}_p$ and $\boldsymbol{a}_p$, with $\boldsymbol{e}_p$ given via (6b) (with $v_p = 0$), are then defined via integrals

$$\boldsymbol{b}_p(\boldsymbol{x}_P) = \frac{\mu_0}{4\pi}\int_{\Omega_{s,p}} (\boldsymbol{j}_{s,p}\times\boldsymbol{r})\,/\,r^3\, d\boldsymbol{x}_Q\,, \tag{11a}$$

$$\boldsymbol{a}_p(\boldsymbol{x}_P) = \frac{\mu_0}{4\pi}\int_{\Omega_{s,p}} \boldsymbol{j}_{s,p}\,/\,r\, d\boldsymbol{x}_Q\,, \tag{11b}$$

with $\boldsymbol{x}_P \in \Omega_p$ the calculation point position vector, $\boldsymbol{x}_Q \in \Omega_{s,p}$ the integration point position vector and $r = \boldsymbol{x}_P - \boldsymbol{x}_Q$. The source fields are to be calculated afterward only in some particular regions, for a change to a volume conductor or when adding other regions.

When used as a VS in a region $\omega_{s,p} \subset \Omega_p$ for an SP p, a Biot-Savart source, $\boldsymbol{a}_{q,BS}$ from (11b), gains at being projected only on the boundary $\partial\omega_{s,p}$ of $\omega_{s,p}$ via

$$(\boldsymbol{a}_{q,p-mesh}, \boldsymbol{a}')_{\partial\omega_{s,p}} = (\boldsymbol{a}_{q,BS}, \boldsymbol{a}')_{\partial\omega_{s,p}}, \forall \boldsymbol{a}' \in F_p^1(\partial\omega_{s,p}). \tag{12}$$

Then, its surface projection $\boldsymbol{a}_{q,p\text{-}mesh}|_{\partial\omega_{s,p}}$ defines a BC for a physical problem of form (1)-(3) in $\omega_{s,p}$, with the weak form (8) here reduced to

$$(\mu_q^{-1}\,\mathrm{curl}\,\boldsymbol{a}_{q,p-mesh}, \mathrm{curl}\,\boldsymbol{a}')_{\omega_p} = 0\,, \forall \boldsymbol{a}' \in F_p^1(\omega_{s,p})\,, \tag{13}$$

to determine the volume extension $\boldsymbol{a}_{q,p\text{-}mesh}|_{\omega_{s,p}}$. In this way, the heavy Biot-Savart evaluation that would be needed at each Gauss point in (9) is avoided and replaced by a physical problem solution of similar computational weight. From $\boldsymbol{a}_{q,p\text{-}mesh}|_{\omega_{s,p}}$, both $\boldsymbol{b}_{q,p\text{-}mesh}|_{\omega_{s,p}}$ and $\boldsymbol{e}_{q,p\text{-}mesh}|_{\omega_{s,p}}$ can be determined for VSs (4a-b), thus with no need to separately evaluate (11a-b).

B. Perfect Magnetic Material BC (region-PMBC)

An SP $p \equiv$ *region-PMBC* is defined in a new domain Ω_p by considering some added magnetic regions $\Omega_{r,p,i}$ (i is the region index; $\Omega_{r,p,i} \subset \Omega_{c,p}^{\,C}$ or $\Omega_{r,p,i} \subset \Omega_{c,p}$) as being perfect, with infinite permeability ($\mu_p \to \infty$) [1]. Its solution can serve as a reference solution for any finite μ_p further considered. The interior of $\Omega_{r,p,i}$, with zero magnetic field $\boldsymbol{h}_p$ inside, is extracted from the studied domain Ω_p and treated in (8) via BC (3a) fixing a zero trace of total magnetic field $\boldsymbol{h} = \boldsymbol{h}_p + \Sigma_{q<p}\boldsymbol{h}_q$ on boundaries $\Gamma_{r,p,i} = \partial\Omega_{r,p,i}$, thus coupling both the unknown fields and the fields from previous SPs q, $\forall\, q < p$, acting as weak SSs via (10), i.e.

$$\boldsymbol{n}\times\boldsymbol{h}_p|_{\Gamma_{r,p,i}} = -\sum\nolimits_{q<p} \boldsymbol{n}\times\boldsymbol{h}_q|_{\Gamma_{r,p,i}}\,. \tag{14}$$

A non-zero trace $\boldsymbol{n}\cdot\boldsymbol{b}_p|_{\Gamma_{r,p,i}}$ will be part of the solution of (8), thus giving a discontinuity $[\boldsymbol{n}\cdot\boldsymbol{b}_p]_{\Gamma_{r,p,i}} = \boldsymbol{n}\cdot\boldsymbol{b}_p|_{\Gamma_{r,p,i}}$ to be further considered as a strong SS for a correction SP.

C. Perfect Conductor BC (region-PCBC)

An SP $p \equiv$ *region-PCBC* is defined in Ω_p by considering some added conductors $\Omega_{c,p,i}$ (i is the conductor index) as being perfect, with $\sigma_p \to \infty$ [1]-[2] (Fig. 1). Its solution, independent of the conductivity, can serve as a reference solution for any finite conductivity further considered. This results in a zero skin depth and surface currents. The interior of $\Omega_{c,p,i}$, with zero fields inside, is extracted from the studied domain Ω_p and treated in (8) via BCs (3b) fixing a zero trace of total magnetic flux density $\boldsymbol{b} = \boldsymbol{b}_p + \Sigma_{q<p}\boldsymbol{b}_q$ on boundaries $\Gamma_{c,p,i} = \partial\Omega_{c,p,i}$. This thus couples both the unknown $\boldsymbol{b}_p$ and the fields from previous SPs q, $\forall\, q < p$, acting as SSs [1]-[2], [5]-[6], i.e.

$$\boldsymbol{n}\cdot\boldsymbol{b}_p|_{\Gamma_{c,p,i}} = -\sum\nolimits_{q<p} \boldsymbol{n}\cdot\boldsymbol{b}_q|_{\Gamma_{c,p,i}}\,, \tag{15a}$$

or, in terms of the primal unknown $\boldsymbol{a}_p$, with the strong BC

$$\boldsymbol{n}\times\boldsymbol{a}_p|_{\Gamma_{c,p,i}} = \boldsymbol{n}\times\mathrm{grad}\,w_p|_{\Gamma_{c,p,i}} - \sum\nolimits_{q<p} \boldsymbol{n}\times\boldsymbol{a}_q|_{\Gamma_{c,p,i}}\,, \tag{15b}$$

with w_p an unknown surface scalar potential; explicitly defining w_p instead of $\boldsymbol{a}_p$ on $\Gamma_{c,p,i}$ fixes (15a). A non-zero trace $\boldsymbol{n}\times\boldsymbol{h}_p|_{\Gamma_{c,p,i}}$ will be part of the solution of (8), thus giving a discontinuity $[\boldsymbol{n}\times\boldsymbol{h}_p]_{\Gamma_{c,p,i}} = \boldsymbol{n}\times\boldsymbol{h}_p|_{\Gamma_{c,p,i}}$ to be further considered as a weak SS for a correction SP.

D. Impedance BC (region-IBC)

In an SP $p \equiv$ *region-IBC*, some conductors can also be extracted from Ω_p by using IBCs relating the tangential traces of total magnetic and electric fields on their boundaries $\Gamma_{c,p,i}$ (actually the outer boundary $\Gamma_{c,p,i}^+$ of $\Omega_{c,p,i}$) [5]-[6] (Figs. 1 and 3), thus also coupling both unknown and previous (as SSs) solutions q, via the BC

$$\boldsymbol{n} \times \boldsymbol{h}_p|_{\Gamma_{c,p,i}} = Z_{c,p,i}^{-1}\, \boldsymbol{n} \times (\boldsymbol{n} \times \boldsymbol{e}_p)|_{\Gamma_{c,p,i}} + \sum\nolimits_{q<p} Z_{c,p,i}^{-1}\, \boldsymbol{n} \times (\boldsymbol{n} \times \boldsymbol{e}_q)|_{\Gamma_{c,p,i}} - \sum\nolimits_{q<p} \boldsymbol{n} \times \boldsymbol{h}_q|_{\Gamma_{c,p,i}}, \tag{16}$$

with $Z_{c,p,i}$ the surface impedance for conductor $\Omega_{c,p,i}$, i.e.,

$$Z_{c,p,i} = (\sigma_p \delta_p)^{-1} (1+j), \text{ with } \delta_p = \sqrt{2/(\omega \sigma_p \mu_p)}, \tag{17a-b}$$

with ω the angular frequency ($\omega = 2\pi f$, with f the frequency) and j the imaginary unit ($\partial_t \equiv j\omega$ in the frequency domain); δ_p is the skin depth. BC (16) is then to be expressed in (8), with $\Gamma_{c,p,i} \subset \Gamma_{h,p} \backslash \gamma_p$, in terms of the trace of the primal unknown $\boldsymbol{a}_p$ with

$$\boldsymbol{n} \times (\boldsymbol{n} \times \boldsymbol{e}_p)|_{\Gamma_{c,p,i}} = (\boldsymbol{n} \times (\partial_t \boldsymbol{a}_p + \boldsymbol{u}_p)) \times \boldsymbol{n}|_{\Gamma_{c,p,i}}. \tag{18}$$

The solution of (8) in this SP contains non-zero traces $\boldsymbol{n} \times \boldsymbol{h}_p|_{\Gamma_{c,p,i}}$ and $\boldsymbol{n} \times \boldsymbol{a}_p|_{\Gamma_{c,p,i}}$ on $\Gamma_{c,p,i}^+$. The traces on the inner boundary $\Gamma_{c,p,i}^-$ being zero (the IBC model implying zero inner volume fields), trace discontinuities through the resulting double layer $\Gamma_{c,p,i}$ thus occur. They can further define weak and strong SSs for a correction SP.

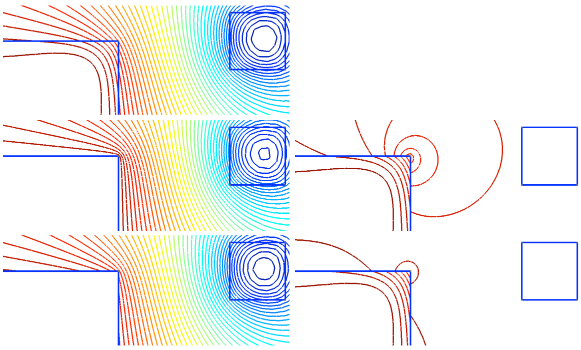

Fig. 1. Field lines near a conductor corner, *from top to bottom:* complete solution, *left:* CORE-PCBC, CORE-IBC models, *right:* associated volume corrections CORE-VOL-SS; same scale for all maps to point out the decrease of the required correction [6].

E. Volume Region from VSs (region-VOL-VS)

A volume region $\Omega_{c,p,i} \subset \Omega_{c,p}$ is considered in an SP $p \equiv$ *region-VOL-VS* (Fig. 2) via the VSs (4a-b) [3], [5]-[6] using all previous solutions q, $\forall\, q < p$, i.e.

$$\boldsymbol{h}_{s,p} = (\mu_p^{-1} - \mu_{p-1}^{-1}) \sum\nolimits_{q<p} \boldsymbol{b}_q, \tag{19a}$$

$$\boldsymbol{j}_{s,p} = (\sigma_p - \sigma_{p-1}) \sum\nolimits_{q<p} \boldsymbol{e}_q, \tag{19b}$$

where μ_{p-1} and σ_{p-1} are the lastly considered material characteristics before their changes to these of the actual conductor.

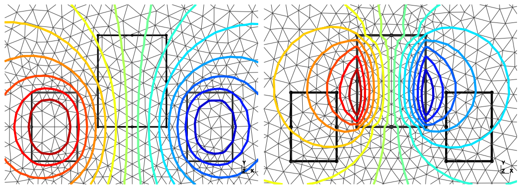

Fig. 2. Field lines for an inductor alone COND-FE ($\boldsymbol{b}_1$, *left*) and for the added core CORE-VOL-VS ($\boldsymbol{b}_2$, $\mu_{r,core} = 100$) (*right*); distinct meshes are used for problems 1 and 2 [3].

F. Volume Region from SSs (region-VOL-SS)

In case previous solutions q aimed at zeroing the fields in $\Omega_{c,p,i}$, e.g., with $\Omega_{c,p,i}$ previously considered via PMBC, PCBC or IBC (Figs. 1, 3, 4 and 5), the VSs in (19a-b) are zero. In such cases, all the fields being carried in the double layer of its boundary, trace discontinuities of both $\boldsymbol{h}_q$ and $\boldsymbol{e}_q$ ($\boldsymbol{a}_q$) occur. Their opposite values then define SSs for SP p in (5a), weakly expressed via (10), and (5b) (and (7b)), strongly expressed in function space $F_p^1(\Omega)$.

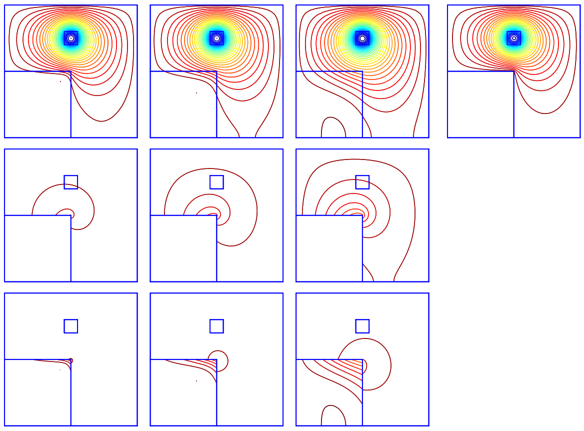

Fig. 3. Field lines near a conductor corner for different frequencies ($f = 12.5$ kHz (*column 1*); $f = 3.125$ kHz (*column 2*), $f = 0.781$ kHz (*column 3*)), *from top to bottom:* complete solutions, CORE-PCBC initial solution (*row 1, column 4*), CORE-IBC correcting CORE-PCBC, CORE-VOL-SS corrections showing field discontinuities at core interface ($\mu_{r,core} = 1$, $\sigma_{core} = 10^6$ S/m); same scale for direct comparisons [6].

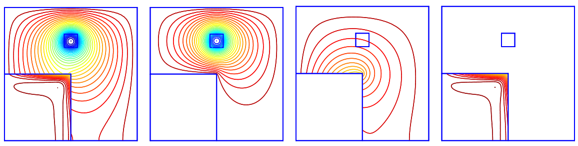

Fig. 4. Field lines near a conductive magnetic core, *from left to right:* complete solution, CORE-PCBC initial solution, CORE-IBC correcting CORE-PCBC, CORE-VOL-SS correction ($\mu_{r,core} = 16$, $\sigma_{core} = 10^6$ S/m, $f = 0.781$ kHz, $\delta = 4.5$ mm); same scale for direct comparisons [6].

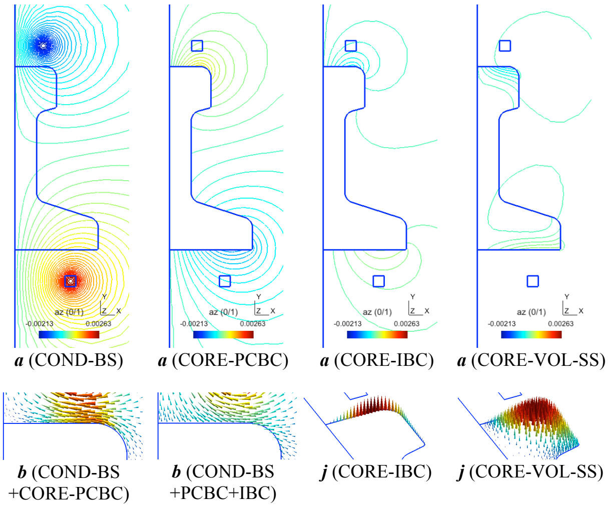

Fig. 5. Field lines (***a***), magnetic flux density (***b***) and eddy current density (***j***) in a 2-D rail induction heating system for progressive SPs (COND-BS, CORE-PCBC, CORE-IBC, CORE-VOL-SS); $f = 1$ kHz, $\mu_r = 1$, d = 16 mm [5].

Another mean to avoid VSs and to solely use SSs is via the general method described hereafter, which usually strongly lightens the computational process. A previous model of $\Omega_{c,p,i}$ could be a Biot-Savart filament model (e.g., wire conductor) [11] or an homogenized model using equivalent material properties (e.g., coil, foil winding, lamination stack).

Corrections can be done for the whole volume region or some of its portions, e.g., a selection of conductors in a coil or in a lamination stack where significant edge effects can occur. Subdomain $\Omega_{vol,p}$ denotes the region to correct (Fig. 6) which is now defined with its actual volume, made of both conducting and non-conducting materials (e.g., conductors and insulations), that can be finely meshed, and its surrounding $\Omega_{vol,p}{}^{C}$ is kept homogenized, thus coarsely meshed. The correction solution is calculated via an SP p in $\Omega_p = \Omega_{vol,p} \cup \Omega_{vol,p}{}^{C}$ with adequate sources. The key is to suppress the previous solution in $\Omega_{vol,p}$ while keeping it unchanged outside (SP pa), simultaneously with the consideration of the actual μ_p and σ_p in $\Omega_{vol,p}$ (SP pb). This is done by defining both tangential and normal trace discontinuities of the correction field through the boundary of $\Gamma_{vol,p} = \partial\Omega_{vol,p}$ as SSs equal to the corresponding traces of the previous solution q along $\Gamma_{vol,p}$ (that can exist or not in SP q) , i.e.,

$$[\boldsymbol{n} \times \boldsymbol{h}_p]_{\Gamma_{vol,p}} = \boldsymbol{n} \times \boldsymbol{h}_q|_{\Gamma_{vol,p}} \,, \quad [\boldsymbol{n} \cdot \boldsymbol{b}_p]_{\Gamma_{vol,p}} = \boldsymbol{n} \cdot \boldsymbol{b}_q|_{\Gamma_{vol,p}} \,. \qquad \text{(20a-b)}$$

This requires a mesh projection of solution q in a layer of FEs along the boundary of $\Omega_{vol,p}$. Each volume correction thus gives the total field in $\Omega_{vol,p}$, is discontinuous through its boundary and quickly decreases outside (Figs. 7, 8, 9, 10, 11), which justifies the use of a coarse mesh in the outer region.

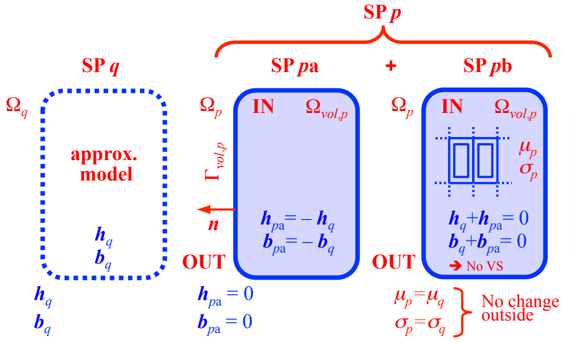

Fig. 6. From an approximate model (SP q) to a fine volume (SP p) FE representation of a conductor: SP p is split into SPs pa and pb, simultaneously solved, SP pa removing the volume solution q inside the conductor and SP pb considering the actual volume conductor properties (of all its subregions), with no need of VSs for change of properties, but with SSs for unified SP p.

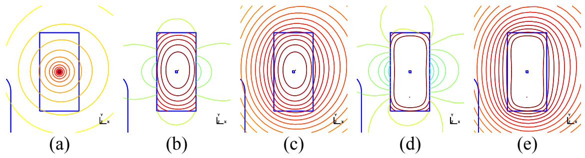

Fig. 7. Field lines in the surrounding of an inductor (portion of a full geometry, wire position shown): (a) Biot-Savart field from all wire inductors COND-BS ($\boldsymbol{b}_1$, actually not calculated in the whole domain), (b-c) static volume correction COND-VOL-SS ($\boldsymbol{b}_{2,sta}$) and total field, (d-e) dynamic volume correction COND-VOL-SS ($\boldsymbol{b}_{2,dyn}$) and total field. The volume correction gives the total field in the volume inductor, is discontinuous through the inductor boundary and quickly decreases outside [11].

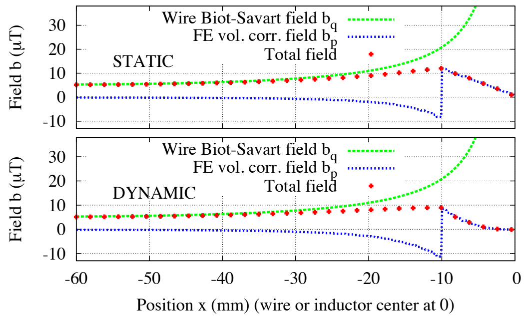

Fig. 8. Magnetic flux density versus distance from conductor (half-width in [−10,0] mm): wire conductor Biot-Savart field COND-BS, FE volume correction COND-VOL-SS and total fields (static and dynamic problems) [11].

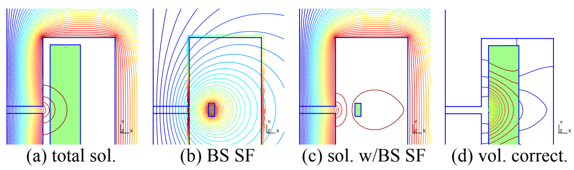

Fig. 9. Current source in a slot with air gap: field lines for (a) full model solution, (b) BS SF with its projection limited to the core boundary (COND-BS), (c) total solution with BS SF, (d) volume correction of coil and its surrounding (COND-VOL-SS), pointing out the field trace discontinuities.

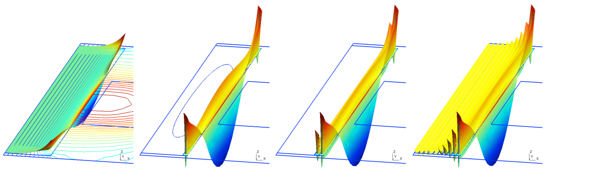

(a) (b) (c) (d)

Fig. 10. Lamination stack (half core, number of lam. = 10, lam. thickness 0.5 mm, insulation 20 μm, $\mu_{r,lam} = 2500$, $\sigma_{lam} = 5\ 10^6$ S/m; with air gaps, for longitudinal and transverse fluxes): homogenized solution (a) and corrected solutions CORE-VOL-SS in 1 (b), 2 (c) and all laminations (d) (frequency 1 kHz) (field lines; eddy current density in elevation).

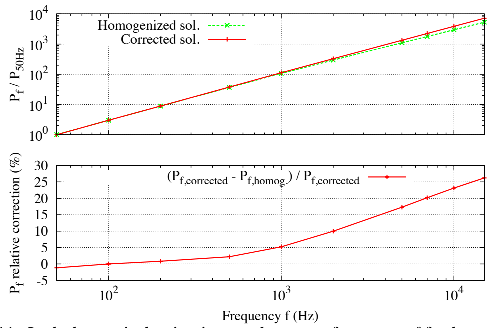

Fig. 11. Joule losses in lamination stack versus frequency *f* for homogenized and corrected solutions: ratio (in log scale) with losses at 50Hz (*top*), relative correction strongly increasing with *f* (*bottom*), pointing out its importance.

G. *Inductance and resistance calculation*

The self inductance of a BS conductor, and the possible mutual inductances with other BS conductors, can be calculated via double integral Neumann formulas [8]-[9]. The resistance can be approximated as well (Fig. 11). After a volume correction SP *p*, the corrected inductance is advantageously obtained with the solution $\boldsymbol{a}_p$ only in $\Omega_{s,p}$ and $\Omega_{c,p}$, i.e., via

$$\Phi_{s,p} = (\boldsymbol{j}_{s,p}, \boldsymbol{a}_p)_{\Omega_{s,p}}, \quad \Phi_{c,p} = (\boldsymbol{j}_p, \boldsymbol{a}_p)_{\Omega_{c,p}}, \qquad (21a\text{-}b)$$

defining the total linkage magnetic fluxes $\Phi_{s,p}$ and $\Phi_{c,p}$ [4], thus as the new global value without any reference to the BS inductance approximation. This is a valuable key feature of the proposed SPM.

An added region in an SP gives an inductance change that is calculated by a volume integral limited to the added region (via the reciprocity theorem [7]), which is another key advantage of the SPM.

IV. Conclusion

The developed FE-SPM allows to split magnetodynamic problems, gathering active and passive conductors and magnetic regions, into SPs of lower complexity regarding meshing operations and computational aspects, with reuse of shared solutions. Each considered region, with its surrounding, is defined with its proper FE mesh, and gives its contributions to the total solution, mainly as source and reaction fields. With the SPM, the source fields are efficiently defined so as to act in reduced supports for the reaction field calculation, which is of particular importance for Biot-Savart models. A source field proper to one region can be used as a source not only for another region but also for an improved model of this source region, which is of interest for model improvements, e.g., from Biot-Savart wire models to FE volume models of conductors, or from homogenized FE models to fine FE models. Each reaction field can become a source field for its own region or other regions. Progressive corrections can be done from static to dynamic models, thus for accurate skin and proximity effects. The proposed approach allows to go one step further than the classical method using Biot-Savart source fields, offering the possibility to focus afterwards on the actual volume conductor with FEs, with a local refined mesh, not only in statics but also in dynamics. Accurate determination of inductances, resistances, Joule losses and forces can thus be obtained in a large frequency range. The method, tested in 2-D, is directly applicable in 3-D.

References

[1] P. Dular, R.V. Sabariego and L. Krähenbühl, “Subdomain Perturbation Finite-Element Method for Skin and Proximity Effects”, IEEE Trans. Magn., vol. 44, no. 6, pp. 738-741, 2008.

[2] P. Dular, R. V. Sabariego, L. Krähenbühl. “Subdomain perturbation finite element method for skin and proximity effects in inductors,” *COMPEL*, Vol. 27, No. 1, pp. 72-84, 2008.

[3] P. Dular, R. V. Sabariego, C. Geuzaine, M. V. Ferreira da Luz, P. Kuo-Peng and L. Krähenbühl, “Finite Element Magnetic Models via a Coupling of Subproblems of Lower Dimensions,” *IEEE Trans. Magn.*, vol. 46, no. 8, pp. 2827-2830, 2010.

[4] P. Dular, L. Krähenbühl, R.V. Sabariego, M. V. Ferreira da Luz, P. Kuo-Peng, C. Geuzaine. “A finite element subproblem method for position change conductor systems,” *IEEE Trans. Magn.*, vol. 48, no. 2, pp. 403-406, 2012.

[5] P. Dular, V. Péron, L. Krähenbühl, C. Geuzaine. “Progressive Eddy Current Modeling via a finite element subproblem method,” *Proceedings of ISEF 2013 (International Symposium on Electromagnetic Fields in Mechatronics, Electrical and Electronic Engineering)*, paper OS5-279_1/6, 6 pp., 2013.

[6] P. Dular, V. Péron, R. Perrussel, L. Krähenbühl, C. Geuzaine. “Perfect conductor and impedance boundary condition corrections via a finite element subproblem method,” *IEEE Trans. Magn.*, vol. 50, no. 2, paper 7000504, 4 pp., 2014.

[7] Z. Badics, Y. Matsumoto, K. Aoki, F. Nakayasu, M. Uesaka, K. Miya, “An effective 3-D finite element scheme for computing electromagnetic field distorsions due to defects in eddy-current nondestructive evaluation,” *IEEE Trans. Magn.*, Vol. 33, No. 2, pp. 1012-1020, 1997.

[8] R. Dengler, “Self inductance of a wire loop as a curve integral,” *arXiv:1204.1486 [physics.class-ph]*, 14 pp., 2013.

[9] C. Dumont de Chassart, M. Van Beneden, V. Kluyskens, B. Dehez, “Fully analytical determination of inductances in windings with axial and azimuthal wires”, *Proceedings of ISEF 2013 (International Symposium on Electromagnetic Fields in Mechatronics, Electrical and Electronic Engineering)*, paper PS2-074_1/7, 7 pp., 2013.

[10] C. Geuzaine, B. Meys, F. Henrotte, P. Dular, W. Legros, “A Galerkin projection method for mixed finite elements,” *IEEE Trans. Magn.*, Vol. 35, No. 3, pp. 1438-1441, 1999.

[11] P. Dular, V. Péron, L. Krähenbühl, C. Geuzaine. “Subproblem Finite Element Refinement of Inductors from Wire to Static and Dynamic Volume Models,” *Proceedings of CEFC 2014, Annecy, May 2014*.